Mass collection of magnetotactic bacteria from the permanently stratified ferruginous Lake Pavin, France

Vincent Busigny, François P Mathon, Didier Jézéquel, Cécile C Bidaud, Eric Viollier, Gérard Bardoux, Jean-jacques Bourrand, Karim Benzerara, Elodie Duprat, Nicolas F Menguy, et al.

Mass collection of magnetotactic bacteria from the permanently stratified ferruginous Lake Pavin, France

Vincent Busigny[1,2,*], François P. Mathon[1,3], Didier Jézéquel[1,4], Cécile C. Bidaud[5], Eric Viollier[1], Gérard Bardoux[1], Jean-Jacques Bourrand[1], Karim Benzerara[5], Elodie Duprat[5], Nicolas Menguy[5], Caroline L. Monteil[3], Christopher T. Lefevre[3,*]

[1]Université de Paris, Institut de Physique du Globe de Paris, CNRS, F-75005, Paris, France

[2]Institut Universitaire de France, 75005 Paris, France

[3]Aix-Marseille University, CNRS, CEA, UMR7265 Institute of Biosciences and Biotechnologies of Aix-Marseille, CEA Cadarache, F-13108 Saint-Paul-lez-Durance, France

[4]INRAE & Université Savoie Mont Blanc, UMR CARRTEL, 74200 Thonon-les-Bains, France

[5]Sorbonne Université, Muséum National d'Histoire Naturelle, UMR CNRS 7590, IRD. Institut de Minéralogie, de Physique des Matériaux et de Cosmochimie (IMPMC), Paris, France.

*For correspondence. E-mails: busigny@ipgp.fr, christopher.lefevre@cea.fr

Abstract

Obtaining high biomass yields of specific microorganisms for culture-independent approaches is a challenge faced by scientists studying organisms recalcitrant to laboratory conditions and culture. This difficulty is highly decreased when studying magnetotactic bacteria (MTB) since their unique behavior allows their enrichment and purification from other microorganisms present in aquatic environments. Here, we use Lake Pavin, a permanently stratified lake in the French Massif Central, as a natural laboratory to optimize collection and concentration of MTB that thrive in the water column and sediments. A method is presented to separate MTB from highly abundant abiotic magnetic particles in the sediment of this crater lake. For the water column, different sampling approaches are compared such as *in situ* collection using a Niskin bottle and online pumping. By monitoring several physicochemical parameters of the water column, we identify the ecological niche where MTB live. Then, by focusing our sampling at the peak of MTB abundance, we show that the online pumping system is the most efficient for fast recovering of large volumes of water at a high spatial resolution, which is necessary considering the sharp physicochemical gradients observed in the water column. Taking advantage of aerotactic and magnetic MTB properties, we present an efficient method for MTB concentration from large volumes of water. Our methodology represents a first step for further multidisciplinary investigations of the diversity, metagenomic and ecology of MTB populations in Lake Pavin and elsewhere, as well as chemical and isotopic analyses of their magnetosomes.

Introduction

The recent technological advances are increasingly allowing the study of microorganisms using culture-independent approaches in many fields of research. These advances include the development of tools to analyze genomes at the single cell scale, as well as the ultrastructure and/or chemistry of microorganisms (Blainey, 2013). However, some analytical approaches still require high biomass and thus often rely on cultured microorganisms or natural enrichment (*e.g.* bloom). Magnetotactic bacteria (MTB) represent one example of microorganisms at the origin of numerous interdisciplinary studies using culture-independent approaches over the last decades mainly because most strains are recalcitrant to growth (Abreu *et al.*, 2007; Lefèvre and Bazylinski, 2013; Lin *et al.*, 2017). For instance, significant progress has been achieved on MTB diversity, chemistry and magnetosome biomineralization based on culture-independent approaches such as single-cell analysis (Jogler *et al.*, 2010; Kolinko *et al.*, 2016), coupled FISH-SEM/TEM (Li *et al.*, 2017, 2019; Koziaeva *et al.*, 2020; Liu *et al.*, 2020; Qian *et al.*, 2020), comprehensive TEM (Li *et al.*, 2015; Zhang *et al.*, 2017; Li *et al.*, 2020a; Li *et al.*, 2020b) and the combination of TEM and synchrotron-based STXM (Li *et al.*, 2020c). MTB can be concentrated and purified magnetically from natural aquatic environments thanks to their magnetosome chain at the origin of their magnetotactic behavior (Bazylinski and Frankel, 2004). Magnetosomes are membrane-enveloped ferrimagnetic nanocrystals, which serve as magnetic field sensors (Blakemore, 1975). Their alignment in linear chains imposes a magnetic moment to the bacteria, which ensures navigation in the weak geomagnetic field along vertical redox gradients (Bazylinski and Frankel, 2004). This behavior, named magnetotaxis, is based on MTB chemo-aerotactic capability and active swimming motility. It likely represents a selective fitness advantage in their natural habitat, which is the oxic-anoxic transition zone (OATZ) of aquatic ecosystems. Most cultured MTB are micro-aerophilic (Lefèvre *et al.*, 2014). Consequently, sampling for MTB is generally based on the collection of sediment or water samples that comprise the OATZ. MTB present in sediments can be sampled from the shore

(Liu *et al.*, 2018), by free diving (Lefèvre *et al.*, 2009), or using a bottom sampler (Kolinko *et al.*, 2013). In contrast, MTB present in the water column of stratified ecosystems have previously been collected using Geopump peristaltic pump (Simmons *et al.*, 2004; Moskowitz *et al.*, 2008), Niskin bottle (Rivas-Lamelo *et al.*, 2017), free-flow bottle or automatic flow injection sampler (Schulz-Vogt *et al.*, 2019).

Their detection in environmental water and sediment samples is relatively easy due to their magnetotactic behavior. Indeed, MTB can be enriched magnetically by placing a bar magnet adjacent to the outer wall of a bottle filled with environmental sample. If MTB are abundant in the sample, a brownish or grayish-to-white spot containing mainly MTB will form next to the inside of the glass wall closest to the bar magnet. Cells can be easily harvested from the bottle and examined using light microscopy. Few improvements of the magnetic concentration of MTB have been proposed such as (i) a glass apparatus containing a capillary end allowing the concentration of MTB from a large volume of sediment when the apparatus is introduced in a coiled tube that generates a homogenous magnetic field (Lins *et al.*, 2003), (ii) an apparatus containing a separating chamber for an initial enrichment of MTB and a sampling chamber where MTB are further concentrated and harvested (Xiao *et al.*, 2007), (iii) a "MTB trap" where south- and north-seeking MTB are magnetically directed toward the tips of collection tubes, from which they can be conveniently collected for further analyses (Jogler, Lin, *et al.*, 2009) and (iv) a MTB column separation, the MTB-CoSe method, that allows collection of magnetotactic cells directly from sediment samples (Koziaeva *et al.*, 2020). The modification of the techniques commonly used for sampling and observation of environmental magnetotactic microorganisms recently allowed to extend our knowledge of the diversity and ecology of magnetotaxis in bacteria (Lin *et al.*, 2018; Monteil and Lefevre, 2019; Monteil *et al.*, 2019, 2021; Koziaeva *et al.*, 2020). Even if all these techniques allow to get biological material in sufficient concentrations for biodiversity studies, the abundance of bacterial populations recovered is not high enough to properly investigate some important magnetic, chemical and

97 isotopic features of the magnetic minerals they form. These aspects are yet essential to
98 understand the molecular and geochemical biomineralization processes. Indeed, the separation
99 of magnetite from MTB in the laboratory for subsequent Fe isotope analyses requires a
100 minimum of 0.1 mg of magnetite (Amor *et al.*, 2016, 2018). This represents a total amount of
101 MTB of ~10^{10} cells, assuming typically 30 magnetosomes per cell and a magnetosome length
102 of 50 nm. To improve our ability to harvest large amount of MTB from natural environment
103 for multidisciplinary studies, including biological, mineralogical and geochemical analyses, we
104 tested and optimized several approaches to collect and concentrate MTB.
105 Lake Pavin (Massif Central, France) was selected as a natural laboratory for the following
106 reasons: (i) it is a ferruginous meromictic lake, *i.e.* permanently stratified with an OATZ located
107 in the water column instead of the sediment (Michard *et al.*, 1994; Aeschbach-Hertig *et al.*,
108 1999, 2002); (ii) the physicochemical conditions of the lake and associated sediments have been
109 studied extensively, and geochemical cycles are well constrained (Michard *et al.*, 1994; Viollier
110 *et al.*, 1995; Albéric *et al.*, 2000; Schettler *et al.*, 2007; Assayag *et al.*, 2008; Busigny *et al.*,
111 2014; Cosmidis *et al.*, 2014) and (iii) recent exploratory field trips at Lake Pavin demonstrated
112 that MTB are exceptionally abundant in concentration and biodiversity in the water column and
113 sediments and may contribute to the geochemical cycles of P, Ca and C (Miot *et al.*, 2016;
114 Rivas-Lamelo *et al.*, 2017; Monteil *et al.*, 2021).
115 Lake Pavin is the youngest crater lake of the Massif Central volcanic area (about 7000 years
116 cal BP) (Chapron *et al.*, 2010). It is redox-stratified, with anoxic and ferruginous deep waters
117 extending between 50-55 and 92 m in depth (monimolimnion), and topped by oxic waters
118 (mixolimnion) (Cosmidis *et al.*, 2014; Rivas-Lamelo *et al.*, 2017; Berg *et al.*, 2019). The
119 position of the OATZ varies slightly with time in a depth range comprised between 50 and 60
120 m (Michard *et al.*, 1994; Cosmidis *et al.*, 2014; Rivas-Lamelo *et al.*, 2017; Berg *et al.*, 2019).
121 In the deep waters, ferrous iron ($Fe(II)_{aq}$) along with NH_4^+, are the main dissolved cations, with
122 concentrations up to 1 mM (Michard *et al.*, 1994; Viollier *et al.*, 1995; Busigny *et al.*, 2014,

2016). Iron is efficiently confined below the oxic-anoxic boundary due to the formation of insoluble ferric iron species, $Fe(III)_s$, by oxidation with O_2 and other oxidants in the mixolimnion (*e.g.*, NO_3^-, Mn^{4+}) (Lopes *et al.*, 2011). The $Fe(III)_s$ particles settle down and are reduced to soluble $Fe(II)_{aq}$ in the anoxic waters and at the lake bottom by reaction with organic matter. Dissolved $Fe(II)_{aq}$ then diffuses upward in the water column and is finally re-oxidized to Fe(III) at the redox boundary. This process, known as the "iron wheel" has been described in details from available data for dissolved and particulate matter in the water column, settling particles collected by sediment traps and sediment cores (Cosmidis *et al.*, 2014; Busigny *et al.*, 2016). Additionally, the lake's water column has remarkably low sulfate concentrations (< 20 µM), which also keep low level of sulfides (Bura-Nakic *et al.*, 2009). The redox boundary fed by a downward flux of dissolved O_2 and other oxidants, and an upward flux of dissolved Fe(II) represents ideal conditions for magnetosome formation by MTB, as observed in similar stratified aquatic environments (Simmons *et al.*, 2004; Schulz-Vogt *et al.*, 2019).

This contribution first presents a method for sampling MTB from the sediments, with particular emphasis on the separation between MTB and abiotic (volcanic) magnetic particles. Then, the global distribution of MTB in the water column of Lake Pavin is presented. The results of several tests for harvesting MTB from the water column are described and compared, including water sampling using Niskin bottles and online pumping system. Finally, a technique for the concentration and isolation of MTB from a large environmental water volume based on magnetotaxis and chemotaxis is presented. Our results allow the identification of optimal physicochemical parameters for the presence of MTB in the water column. This work is paving the way for future multidisciplinary studies of MTB in Lake Pavin and others natural sites.

Results and discussion

Magnetotactic bacteria are abundant and diverse in the sediments of Lake Pavin

Over the different sampling campaigns performed since 2016 on Lake Pavin, a large abundance (up to 5.8×10^5 cells mL^{-1} of porewater; Monteil *et al.*, 2021) and diversity of MTB morphotypes has been observed in the sediments collected from the shore (Fig. 1). MTB abundance determined in sediments of other aquatic systems generally falls in a range from 10^5 to 10^6 cells mL^{-1} (Spring *et al.*, 1993; Jogler, Kube, *et al.*, 2009) with some studies reporting up to 10^7 cells mL^{-1} (Flies *et al.*, 2005), magnetotactic cocci being in most aquatic habitats the dominant population of MTB. Although only future studies using molecular typing methods will be able to specify the phylogenetic affiliation of these MTB morphotypes, the unique ultrastructure of some of these MTB allows speculations on their taxonomy. First, the recently published calcium-carbonate producing MTB were easy to distinguish thanks to their refractive inclusions, their slow motility and their unique magnetotactic behavior when observed under the light microscope (Figs. 1A and S1A) (Monteil *et al.*, 2021). This MTB morphotype was among the most abundant in sediment samples along with MTB with an ultrastructure typical of the Magnetococcaceae family (*e.g.* coccoid cells, helical motion, two flagella bundles) (Fig. 1B-E) (Bazylinski *et al.*, 2013). Cell's shapes similar to that of *Magnetospirillum* bacteria (*e.g.* thin, *i.e.* < 500 nm, and long, *i.e.* > 5 µm, helical-shaped with one chain of cuboctahedral magnetosomes; Fig. 1F) could also be recognized based on TEM observations (Lefèvre *et al.*, 2012). Rod-shaped MTB producing polyphosphate inclusions very similar to previously described MTB affiliated to the Magnetococcaceae family were also observed (Figs. 1 G and H and S1B) (Spring *et al.*, 1994; Oestreicher *et al.*, 2011; Kolinko *et al.*, 2013). Magnetotactic spirilla very similar (*e.g.* large, *i.e.* between 0.5 and 1 µm, and short, *i.e.* < 3 µm, helical-shaped cells with one chain of prismatic magnetosomes) to described species of the *Magnetospira* genus were also present in sediments of Lake Pavin (Fig. 1I). Then, cells resembling previously described MTB of the Nitrospirae phylum (*e.g.* large rod or ovoid cells with electron dense inclusions and several chain bundles of bullet-shaped magnetosomes) such as *Candidatus* Magnetoovum sp. (Fig. 1J) (Lefèvre *et al.*, 2011; Lin *et al.*, 2012) and *Ca.* Magnetobacterium

bavaricum (Fig. 1K) (Spring *et al.*, 1993; Jogler *et al.*, 2010; Li *et al.*, 2020b) could also be observed (Lefèvre, 2016). Finally, various rods to curved rods producing bullet-shaped magnetosomes were observed and could be tentatively affiliated to the Deltaproteobacteria since their ultrastructure was similar to described magnetotactic species of the *Desulfovibrio* and *Desulfamplus* genera (Fig. 1L-O) (Lefèvre *et al.*, 2016; Descamps *et al.*, 2017; Pan *et al.*, 2019).

Lake Pavin sediments appeared as a natural environment particularly suitable to obtain high MTB biomass. Indeed, after magnetic enrichment of sediment samples using neodymium-iron-boron magnets for 2-3 h, aggregated cells formed a thin irregular whitish pellet measuring up to 5 cm in diameter, containing an estimated number of up to 10^8 magnetotactic cells located against the magnet. However, abiotic magnetic particles were also very abundant in the sediments of this lake and were generally trapped in the pellets during MTB concentration. These abiotic particles were predominantly identified as ilmenite (*i.e.* titanium-iron oxide, $FeTiO_3$) by scanning electron microscopy analyses (Fig. S2). Ilmenite is a slightly magnetic, black and steel-gray mineral. It is a paramagnetic mineral, explaining its attraction during magnetic concentration of Lake Pavin sediments. At the macroscopic scale, it can easily be mistaken with magnetite.

We attempted at purifying a maximum proportion of MTB after their magnetic concentration. Our system, named “migration track”, is similar to the racetrack method developed in previous studies (Wolfe *et al.*, 1987; Li *et al.*, 2010). It improved the purification of north seeking MTB and was used directly on the field (Figs. 2 and S3). The pellets containing abiotic particles, MTB and other microorganisms, were collected with a 1 mL micropipette on the inner wall of the bottles and placed next to the north pole of a strong bar magnet (15 mT at the edge of the drop). Magnetic particles were retained at this extremity while most north-seeking MTB were repulsed and swam in the opposite direction where the south pole of another magnet was placed (3 mT at the edge of the drop). A folded parafilm sheet was used to create a channel filled with

a 0.22-µm-filtered drop of Lake Pavin water overlying the sediments in the sample. Such a protocol avoids the formation of chemical gradients and thus facilitates the northern migration of MTB. The migration time was adjusted in order to obtain a maximum proportion of MTB purified at the extremity of the device. As the majority of MTB were fast swimming bacteria such as magnetotactic cocci with a motility above 200 µm s^{-1}, the drop was spread (*i.e.* 4 to 4.5 cm length) in order to optimize the transfer of magnetotactic cells in the filtered water. Up to 88.0 % (71.9 % in average) of MTB were efficiently purified and concentrated after 60 min of migration in the channel (Fig. 2). A whitish/greyish spot appeared close to the south pole of the magnet where MTB were harvested. A majority of magnetotactic cocci along with other rod-shaped magnetotactic cells composed this pellet containing more than 10^7 cells. This approach combining the standard method for magnetic concentration of sediment samples and our migration track technique allowed us harvesting an important quantity of MTB free of abiotic magnetic particles. These MTB were composed by different populations with proportions likely not representative of their proportions in the environment, as the protocols used for magnetic enrichment and purification do not have the same efficiency for all MTB (e.g. Lin *et al.*, 2008). Purified MTB from dozens of migration track devices were pulled together and concentrated by centrifugation, thus representing a large pellet of purified MTB available for further analyses.

Magnetotactic bacteria are distributed below the oxygen detection limit in the water column of Lake Pavin

Over the different field works in Lake Pavin, the abundance and proportion of the different MTB morphotypes observed in the water column greatly varied depending on the season. Eight MTB morphotypes could be distinguished based on microscopy observations. Among these morphotypes, the most abundant (up to 5.0×10^3 cells mL^{-1}) were cells affiliated to the Magnetococcaceae family that produced polyphosphate inclusions of various sizes along with

various organizations of magnetosomes (Figs. 3A-C and S1C) (Rivas-Lamelo *et al.*, 2017; Liu *et al.*, 2020). MTB producing calcium carbonate inclusions were observed at a lower abundance but could reach a cell density of 4.0×10^2 cells mL^{-1} (Fig. 3D) (Monteil *et al.*, 2021). Two rod-shaped MTB, one producing a single chain of octahedral magnetosomes along with polyphosphate (Figs. 3E and S1C) and the other one producing a single chain of bullet-shaped magnetosomes (Fig. 3F) were also always present in our samples but at a low cell density (< 8 cells mL^{-1}, the lower limit of the technique used to count MTB density using the hanging drop assay). A small vibrio producing one chain of bullet-shaped magnetosomes (Fig. 3G) and some helical MTB resembling cells of the *Magnetospirillum* genus (Fig. 3H) were occasionally observed in samples collected in the water column of Lake Pavin. Other studies on MTB populations living in the water column of stratified aquatic environments also revealed the presence of a majority of magnetotactic cocci affiliated to the Magnetococcaceae family (Simmons *et al.*, 2007; Schulz-Vogt *et al.*, 2019) with abundance up to 3.5×10^6 cells mL^{-1} at the top of the oxycline in Salt Pond, Massachusetts (Simmons *et al.*, 2004, 2007).

From April 2016 to October 2019, ten vertical profiles of MTB distribution along with several physicochemical parameters were obtained across the OATZ of the water column using a Niskin bottle for water collection (Figs. 4 and S4). These profiles could bring important information concerning the MTB distribution in the water column of Lake Pavin. For instance, although there are important variations of the oxygen and redox gradients over the seasons and years, MTB were always distributed below the oxygen detection limit (Figs. 4 and S4). The maximum abundance of MTB in the water column was systematically detected near the maximum decrease of the redox potential, *i.e*. between 51.0 and 57.2 m depth depending on seasons/years (Fig. 4). The peak of turbidity, corresponding mainly to the precipitation of iron phosphate and (oxy)hydroxide (Cosmidis *et al.*, 2014; Busigny *et al.*, 2016), was either at the same depth level as the peak of MTB abundance or just below. In most cases, their depths evolved similarly depending on the season (Figs. 4 and S4). However, it should be noted that

the intensities of the turbidity and MTB peaks did not correlate with each other. For instance, in October 2017, a high MTB concentration of 7.4×10^3 cells mL^{-1} was observed at 51.0 m depth while the peak of turbidity was very weak. Reciprocally, in April 2016, a strong peak of turbidity was observed at 54.6 m depth while the number of MTB reached only 1.4×10^3 cells mL^{-1}. Accordingly, the contribution of MTB populations to the turbidity of the water column is insignificant and the turbidity value cannot be used unequivocally as a proxy for MTB. The peak of MTB was always observed at the level of or below the break of conductivity at value of 78.9 ± 13.0 µS cm^{-1} (n = 10 sampling campaigns using Niskin bottles) which corresponds to the region where iron concentration starts to increase (Cosmidis *et al.*, 2014; Busigny *et al.*, 2016).

In spring and summer, the maximum number of MTB counted in the water column was located between 54.3 and 57.2 m depth, while in autumn, the maximum number of MTB was generally located at a lower depth in the water column, between 51.0 and 53.0 m (Figs. 4B and S5). This zonation can be explained by the dynamics of the upper water column. In winter, shallow waters (0-10 m) cool down and eventually become denser than deeper waters (10 to *ca*. 50-55 m) thus creating an instability and a mixing of the upper water column (*i.e*. mixolimnion). This brings dissolved O_2 to the deep part and slightly deepens the OATZ, turbidity peak and the maximum MTB abundance zone. In contrast, during summer and autumn, shallow waters are warmer and the water column is strongly stratified by the thermocline (*ca*. 8-12 m depth) that limits O_2 renewal in the hypolimnion, inducing an upward shift of chemocline, turbidity and MTB peaks to shallower depth (due to upward Fe(II) diffusion from deep anoxic waters).

Sampling with a Niskin bottle is thus an efficient method to decipher the global distribution of MTB in the water column. Nevertheless, the use of Niskin bottles is associated with several drawbacks. First, the bottles are, in general, vertical and, in our case, with a height of ~50 cm for the 5.7-L bottle and ~100 cm for the 20-L bottle (Fig. 5). As a result, this method provides a limited depth resolution for the assessment of MTB distribution in the water column, not

278 better than 50 to 100 cm. However, near the OATZ of Lake Pavin, the strong stratification at
279 relatively small scale, as measured by *in situ* probes, requires a better depth resolution for water
280 collection. Moreover, water collection takes a long time, especially at a 60 m depth: about 30
281 minutes in total are required for bottle opening, descent, closing, ascent, and emptying on the
282 platform. Then, when a water sample is collected, the only direct control over the depth is a
283 meter counter connected to the pulley of the winch, which provides a poor precision. The depth
284 is precisely known thanks to a depth gauge fixed to the Niskin bottle only when the bottle is
285 pulled out from the water. Thus, there is no direct indication that the bottle is located at the peak
286 of MTB abundance. Therefore, the method of water collection using Niskin bottle is adapted
287 for a study of global MTB distribution in the water column but (i) can hardly target the peak of
288 MTB abundance reproducibly and (ii) cannot be used to establish a precise distribution profile
289 of MTB at high depth resolution.
290
291 ***Online pumping allows a sampling at high depth resolution, showing that MTB distribution***
292 ***is correlated with conductivity and oxygen***
293 We developed an alternative method for water sampling using a vertical graduated pipe settled
294 at depth and connected at the other side of the pipe to a submersible pump (Fig. 5). The water
295 transfer from depth to surface can be rapid and efficient but depends on the pump flow capacity.
296 In the present work, the maximum pump flow reached 8 L min^{-1} (BLDC Pump, model DC50E-
297 1250), filling a 20-L Nalgene bottle in *ca*. 150 s. This is much faster compared to the 30 minutes
298 required to collect 20 L with a Niskin bottle. A clear advantage of our online sampling system
299 is that several Nalgene bottles could be filled from the same depth on a time scale where
300 evolution of the water physico-chemistry and MTB abundance are insignificant. We compared
301 MTB abundances in several Nalgene bottles successively filled and found them statistically
302 identical (data not shown). Moreover, the abundance of cells collected at the same depth using
303 a Niskin bottle was similar or lower compared to our pipe system showing that the flow

generated by the pump has no impact on MTB motility and integrity. Indeed, electron microscopy analyses of cells sampled with the two approaches show similar MTB morphology and magnetosomes organization. For sampling another depth in the water column, the graduated pipe can simply be shifted to a shallower or deeper position. A waiting time is required to flush the water contained in the 60-m-long pipe, corresponding roughly to 150 s. Another benefit of our online sampling system is that it allows the collection of water at relatively high depth resolution of approximately 10 to 20 cm.

In Lake Pavin, although MTB-rich waters can be efficiently collected at a specific depth using our online sampling system, imprecisions persist because the depth of the MTB abundance peak can change over days, and even hours, due to slight variation of the redox boundary and internal waves of the lake (Bonhomme, 2008; Bonhomme *et al.*, 2011). In order to overcome this problem, we evaluated whether physicochemical parameters of the water could be used as a proxy for MTB abundance in the water column. Over several days in July 2019, we monitored MTB cell density around the peak of MTB abundance identified beforehand, as well as temperature, conductivity at 25°C (*i.e.* C_{25}), dissolved oxygen concentration and pH of the water samples (measured *in situ* directly at the extremity of the pipe). The results indicate that MTB cell density ranged from 13 to 1.18×10^4 cells mL^{-1}, temperature from 6.3 to 7.0°C, C_{25} from 63.3 to 78 µS cm^{-1}, and pH from 6.1 to 6.3. Figure 6 illustrates that MTB cell density is not correlated with pH and temperature, but displays specific distribution with C_{25} and dissolved O_2 concentration. MTB cell density tends to increase with decreasing O_2 level, and MTB > 4.0×10^3 cells mL^{-1} are only found when dissolved O_2 is lower than 2 µmol L^{-1}. However, low MTB cell densities are also observed in some water samples with low O_2 (*i.e.* around 2 µmol L^{-1}; Fig. 6A) showing that O_2 concentration is an important parameter controlling MTB distribution but is not sufficient to monitor online MTB abundance. The conductivity is also a relevant parameter since the peak of MTB abundance was systematically

found in a restrictive range of C_{25} values, between 64.7 and 67.1 µS cm^{-1} (Fig. 6B). Considering the twelve richest samples with MTB > 4.0×10^3 cells mL^{-1}, the average C_{25} value is 65.8 ± 1.4 µS cm^{-1} (2σ). The conductivity represents the concentration of dissolved ionic species, including iron. Thus, the peak of MTB abundance in the water column of Lake Pavin occurs at an ideal set of conditions including an oxygen concentration below 2 µmol L^{-1} and a conductivity around 65.8 µS cm^{-1}. The conductivity can be instantaneously measured in the water collected by our online system and was further used as a proxy for MTB abundance.

The MTB abundance, O_2 concentrations and specific conductivity measured along three depth profiles in Lake Pavin water column are reported in Figure 7. While C_{25} showed a progressive increase with depth for the different sampling days, MTB cell density and O_2 concentration showed stronger variabilities and scattering. Oxygen concentration typically decreased with depth but displayed unexpected bursts at depths of 51.5 m (July 14th 2019) and 52.0 m (July 15th 2019). This O_2 increase was not observed in July 17th 2019 although there might be subtle variations at low level. The presence of O_2 anomalies (*i.e.* concentration burst in anoxic waters) may reflect an inflow of a sub-lacustrine intermittent spring, as described previously in Lake Pavin at a depth ranging between 50 and 55 m (Bonhomme *et al.*, 2011). Interestingly, the MTB concentration is anticorrelated with these O_2 burst, with no MTB in elevated O_2 regions (Fig. 7).

Using the online pumping system, we noticed that the MTB abundance exhibited several peaks at different depths in the water column. Two peaks were observed on July 14th and 15th, and three peaks on July 17th (Fig. 7). This was not the case on July 9th and during the other sampling campaigns while performing the MTB abundance profiles with the Niskin bottle. Although MTB are distributed along several meters in the water column, a high depth resolution is thus required to study precisely MTB distribution in the water column of Lake Pavin. The origin of multiple MTB peaks is still poorly constrained. Future studies will have to examine the potential link between physico-chemical conditions and associated MTB populations by monitoring in

detail physico-chemical properties of the water, MTB morphotypes and molecular typing methods.

Finally, two important questions must be discussed concerning our online pumping system. First, when the pipe is left at depth for relatively long time (*e.g*. several minutes or more), where is the water collected at the pipe mouth coming from? It is unknown if the water collected for a long time is derived from a roughly constant depth level, all around, below or above the pipe mouth. Because of strong vertical density gradient in the vicinity of the oxic-anoxic transition zone in Lake Pavin, we can reasonably assume that the zone of water collection around the pipe mouth is similar at each sampling depth (regardless of the water flow direction). This is supported for instance by the progressive increase in conductivity with depth on the different profiles of July 2019 (Fig. 7, in particular the smooth shape of the profiles in July 14^{th} and 15^{th}). The second important question to address is whether the physico-chemical conditions of water are preserved or not during transfer through the pipe from depth to surface. Again, the smooth shape of the conductivity profile suggests that the water was well preserved during ascension. In addition, we noted a clear oxic-anoxic transition of the water samples (even though the oxic zone was not monitored and reported here due to the absence of MTB). The anoxic conditions (*i.e*. below probe detection limit) measured at depth > 52.5 m (Fig. 7) indicate that O_2 diffusion through the pipe did not occur or was negligible during water ascension. The only parameter significantly modified was temperature due to high exchange surface with ambient water around the pipe. The water temperature measured on the platform was between 6.3 and 7°C (Fig. 6), while *in situ* measurement provided values near 4°C. Overall our online pumping system allows to achieve a high spatial resolution together with consistent water conditions and associated MTB abundance.

Chemotaxis and magnetotaxis allow an efficient MTB concentration from large water samples

Most previous studies of environmental MTB focused on water-saturated sediment samples (Jogler *et al.*, 2010; Lefèvre *et al.*, 2011; Lin *et al.*, 2013, 2018) and a few explored the stratified water column of freshwater or saline lakes (Simmons *et al.*, 2004; Rivas-Lamelo *et al.*, 2017; Schulz-Vogt *et al.*, 2019). In all of these studies, MTB were isolated using magnetic enrichment (Jogler and Schüler, 2009; Lefèvre and Bazylinski, 2013; Lin *et al.*, 2017). This magnetotaxis-based procedure is well adapted for samples of small volume (*i.e.* below 1 L) but is not efficient for large volumes such as 10 or 20 L, which are needed for studies that require high MTB biomass, for instance, to combine mineralogical, biological and geochemical analyses of magnetosomes.

In order to concentrate MTB cells from a 20-L volume to 1 L and subsequently perform magnetic enrichment, we explored the possibility to concentrate them using their aerotaxis. Indeed, MTB are known to display strong microaerophilic, aerophilic or -phobic response (Frankel *et al.*, 1997; Lefèvre *et al.*, 2014; Popp *et al.*, 2014). Using our online pumping system, we collected water samples from Lake Pavin (near the peak of MTB abundance) and filled six Nalgene bottles of 20 L each. After sampling, the bottles were left open to air so that O_2 could diffuse into the water (Fig. 8). MTB were expected to swim downwards to the bottom of the bottle. Because O_2 diffusion in water was extremely slow, the experiment was speeded up by gently removing water from the upper part of the bottle by pumping 4 L every 30 or 60 minutes, so that O_2 could diffuse deeper in the bottle while aerotactic cells were swimming downward. Among the six bottles, three of them were pumped every 30 minutes and the three others every 60 minutes. This provided a triplicate of each condition (30 or 60 minutes idle time between pumping). For every volume interval, water was collected and MTB concentration was quantified in triplicate under a light microscope. The distribution of MTB concentration was very consistent and reproducible between triplicates (see error bars on Fig. 8). The results of

the experiment with 30 minutes idle time between pumping showed that MTB swam and concentrated in the bottom water. However, only 42.3 ± 4.1% of the total MTB cells were found in the bottom water (1 L), while ~60% were lost in the upper oxygenated waters. In contrast, the experiment with 60 minutes idle time gave a higher concentration yield with 80.7 (±0.8) % of the total MTB cells present in the bottom water. Overall, this shows that downwards MTB migration imposed by O_2 diffusion in the bottle is an efficient pre-concentration procedure. These data allowed to estimate the motion speed of the slowest MTB from Lake Pavin water column. The vertically travelled distance in the 20 L Nalgene bottle was 10 cm in 60 minutes. This corresponds to MTB motion speed *ca.* 28 μm s^{-1}, which is in the speed range to that previously described for MTB (Lefèvre *et al.*, 2014) and in agreement with light microscope observation where we could distinguish highly motile magnetotactic cocci and some slow motile magnetotactic large rods. A further magnetic enrichment of the chemotactically enriched samples allowed the formation of a large pellet against the magnet that could be easily harvested and used for further analyses of magnetotactic cells or their magnetosomes. For a 20 L bottle sampled at the peak of MTB abundance in Lake Pavin water column, more than 10^8 cells could be collected. Similarly to the magnetic concentration carried out in the sediments, coupling aerotactic and magnetic concentration allows to obtain large pellets of cells composed by several populations of MTB in proportions likely different from the natural ones as the sensitivity to oxygen probably differs between the different MTB present in our samples.

Conclusion

The present work on Lake Pavin provides several analytical methods for optimizing MTB collection in sediments and the water column. In sediments, MTB were efficiently separated from magnetic abiotic particles (*i.e.* volcanic ilmenite) using a “migration track” system, where MTB are left swimming towards a magnet. In the water column, a comparison of sampling protocols based on Niskin bottle and online pumping system demonstrates a stronger potential

of online technique, with fast collection of large volumes (20 L in 150 s) and at high depth resolution (about 10-20 cm). Another strong advantage of the online pumping technique is the capacity to evaluate the zone of maximum MTB abundance using empirical calibration coupling dissolved oxygen and conductivity measurements. While only one peak of MTB was identified on depth profile performed using Niskin bottles, high resolution profile using online pumping system indicates that two to three peaks of MTB are present. Likewise, we anticipate a stratification of MTB morphotypes and a potential link to geochemical parameters in the water column. This aspect will need to be explored in future studies and may help to decipher the ecological niche specific of the different MTB populations present in the water column.

After collection of large volumes of water at depth, MTB can now be efficiently recovered by coupling their aerotactic and magnetic behaviors. This opens a new avenue for chemical and isotopic studies that require large amount of MTB and are usually limited to laboratory cultures. In the case of Lake Pavin, MTB present at the OATZ of the water column show a maximum concentration slightly higher than 10^4 cells mL^{-1}. Therefore, the mass requirement for Fe isotope analysis (~0.1 mg of magnetite, *i.e.* 10^{10} cells) implies that about 1000 L of water will have to be collected and treated. Although this represent a large volume of water, this can reasonably be achieved by the present protocols. The application of these methods to others chemically stratified aquatic environments such as Salt Pond, Massachusetts (Simmons *et al.*, 2004) or the Black Sea (Schulz-Vogt *et al.*, 2019) could be of high interest to carry out a comparative study of MTB ecology, diversity and isotope characteristics from different ecosystems.

Experimental procedures

Sample collection and in situ physicochemical measurements

Sampling in the water column was carried out at ten different dates between April 2016 and October 2019. Samples were collected from a platform located near the center of Lake Pavin

(45.495792°N, 2.888117°E) using a 5.7 L or 20 L Niskin bottle (General Oceanics, USA) connected to a winch or by pumping directly the water using a speed-adjustable 12 V brushless pump (see details in the Results section). For initial MTB counting, water collected at the targeted depths was transferred in one-liter glass bottles filled to their capacity and tightly closed. *In situ* environmental parameters of the water column were acquired with different profiler probes: YSI 6600 (CTD-O_2-pH-ORP), EXO2 (CTD-O_2-pH-ORP-turbidity-chlorophyll-phycocyanine-fDOM), SDOT 300 nke (O_2-T), AQUAlogger 210TYPT Aquatec (turbidity-T-depth), STBD 300 nke (turbidity-T-depth), where CTD stands for conductivity-temperature-depth, ORP for oxidation reduction potential and fDOM for fluorescent dissolved organic matter. Detection limit for dissolved O_2 is *ca*. 0.1% or about 0.3 ± 0.2 µM.

Sediments were sampled along the edge of the dock, near the main access road to Lake Pavin (45.499162°N, 2.886399°E). They were recovered onshore with a scooper by fully filling one-liter glass bottles with 300-400 mL of sediments and overlying 600-700 mL water. During sampling, air bubbles were avoided. Once in the laboratory, bottles were stored with their cap closed, under dim light and at room temperature (~25°C).

Magnetic enrichment and light microscope observation

North-seeking magnetic cells were concentrated by placing the south pole of a magnetic stirring bar or neodymium-iron-boron magnet (disc magnet with a diameter of 5 mm and a height of 5 mm) for 1-3 hours next to the bottle wall, above the sediment-water interface or at mid-height of the water bottle. Examination of magnetically concentrated cells was carried out using the hanging drop technique (Schüler, 2002) under a Zeiss Primo Star light microscope equipped with phase-contrast, differential interference contrast optics and a camera Axiocam 105. Magnetotaxis was evidenced by rotating a stirring bar magnet at 180° on the microscope stage to reverse the local magnetic field.

Cell count profiles

For counting MTB cells in the water column, two 1-L bottles of water were collected at the different investigated depths. For each bottle, three 40-µL drops were immediately observed using the hanging drop technique. Magnetotactic cells accumulated at the edge of the drops when a magnetic field was applied at one side of the drop and were subsequently counted under the light microscope. The counting occurred two minutes after the cells in the hanging drop were exposed to the magnetic field. The number of cells counted in each drop was multiplied by a factor of 25 to obtain the abundance of cells per milliliter. Cell counts were reported as the means of two triplicates counts for each depth. Using this counting method, the lower limit of MTB abundance is 8 cells mL^{-1} (*i.e.* minimum of 1 cell /3 replicates × 25).

Magnetotactic cells in sediment samples were counted using a Malassez counting chamber. Measurements were systematically carried out on three replicates. Cells were not immobilized during counting. Although some MTB are fast swimmers, we were able to count the number of cells in the chamber reproductively. Counts were performed as fast as possible, a task facilitated by the fact that most MTB cells contain refractile inclusions (e.g. sulphur or calcium carbonate) which makes their identification under the microscope easy.

Transmission and scanning electron microscopy (TEM and SEM)

The morphology of MTB as well as the shape and arrangement of magnetosomes were observed after fixation of the cells on a TEM carbon-coated grid. Electron micrographs were recorded with a Tecnai G^2 BioTWIN (FEI Company) equipped with a CCD camera (Megaview III, Olympus Soft imaging Solutions GmbH) using an accelerating voltage of 100 kV. Z-contrast imaging in the high-angle annular dark field (STEM-HAADF) mode, and elemental mapping by X-ray energy-dispersive spectrometry (XEDS) were carried out using a JEOL 2100F microscope. This machine, operating at 200 kV, was equipped with a Schottky emission gun, an ultrahigh resolution pole piece, and an ultrathin window JEOL XEDS detector.

Bulk magnetic particles extracted from the sediments were observed by scanning electron microscopy (SEM) in back-scattered electron and secondary electron imaging modes to characterize both the shape and chemical composition of particles in the samples. Analyses were carried out at Institut de Physique du Globe de Paris (IPGP) using a Carl Zeiss EVO MA10 SEM. Standard operating conditions for SEM imaging and EDS (energy dispersive spectroscopy) analyses were 15 kV accelerating voltage, working distance of 12 mm, and electron beam current of 2-3 nA. Samples were coated with a few nanometers of Au prior to analysis.

Statistical analyses

Statistical analyses were performed in R, version 4.0.0 (R Core Team, 2018). For each variable, groups' averages were compared either by a paired Student's t-test or by a paired non-parametric Mann–Whitney U test if variables were not normally distributed. Differences were considered as significant when P-values were below 0.05.

Acknowledgments

This work was supported by the French National Research Agency (SIGMAG: ANR-18-CE31-0003 and PHOSTORE: ANR-19-CE01-0005), the CNRS: "DEFI Instrumentation aux limites" (MAGNETOTRAP project) and "Programme National Ecosphère Continentale et Côtière (EC2CO)" (BACCARAT2 project – N°13068). C.C. Bidaud was supported by the Frontières de l'Innovation en Recherche et Éducation (FIRE) PhD program from the Centre de Recherches Interdisciplinaires (CRI). Part of this work was supported by IPGP multidisciplinary program PARI and by Region Île-de-France SESAME Grant no. 12015908. We acknowledge the Institut de Radioprotection et de Sûreté Nucléaire (IRSN) at CEA Cadarache for the access of the transmission electron microscope Tecnai G^2 BioTWIN. We would like to thank the town of

Besse for the work facilities in the field, and particularly Marie Léger from the heritage service as well as the technical staff.

References

Abreu, F., Martins, J.L., Silveira, T.S., Keim, C.N., de Barros, H.G.P.L., Filho, F.J.G., and Lins, U. (2007) "Candidatus Magnetoglobus multicellularis", a multicellular, magnetotactic prokaryote from a hypersaline environment. *Int J Syst Evol Microbiol* **57**: 1318–1322.

Aeschbach-Hertig, W., Hofer, M., Kipfer, R., Imboden, D.M., and Wieler, R. (1999) Accumulation of mantle gases in a permanently stratified volcanic lake (Lac Pavin, France). *Geochimica et Cosmochimica Acta* **63**: 3357–3372.

Aeschbach-Hertig, W., Hofer, M., Schmid, M., Kipfer, R., and Imboden, D.M. (2002) The physical structure and dynamics of a deep, meromictic crater lake (Lac Pavin, France). *Hydrobiologia* **487**: 111–136.

Albéric, P., Voillier, E., Jézéquel, D., Grosbois, C., and Michard, G. (2000) Interactions between trace elements and dissolved organic matter in the stagnant anoxic deep layer of a meromictic lake. *Limnology and Oceanography* **45**: 1088–1096.

Amor, M., Busigny, V., Louvat, P., Gélabert, A., Cartigny, P., Durand-Dubief, M., et al. (2016) Mass-dependent and -independent signature of Fe isotopes in magnetotactic bacteria. *Science* **352**: 705–708.

Amor, M., Busigny, V., Louvat, P., Tharaud, M., Gelabert, A., Cartigny, P., et al. (2018) Iron uptake and magnetite biomineralization in the magnetotactic bacterium Magnetospirillum magneticum strain AMB-1: An iron isotope study. *Geochim Cosmochim Acta* **232**: 225–243.

Assayag, N., Jézéquel, D., Ader, M., Viollier, E., Michard, G., Prévot, F., and Agrinier, P. (2008) Hydrological budget, carbon sources and biogeochemical processes in Lac

Pavin (France): Constraints from δ18O of water and δ13C of dissolved inorganic carbon. *Applied Geochemistry* **23**: 2800–2816.

Bazylinski, D.A. and Frankel, R.B. (2004) Magnetosome formation in prokaryotes. *Nat Rev Microbiol* **2**: 217–230.

Bazylinski, D.A., Williams, T.J., Lefèvre, C.T., Berg, R.J., Zhang, C.L., Bowser, S.S., et al. (2013) Magnetococcus marinus gen. nov., sp. nov., a marine, magnetotactic bacterium that represents a novel lineage (Magnetococcaceae fam. nov.; Magnetococcales ord. nov.) at the base of the Alphaproteobacteria. *Int J Syst Evol Microbiol* **63**: 801–808.

Berg, J.S., Jezequel, D., Duverger, A., Lamy, D., Laberty-Robert, C., and Miot, J. (2019) Microbial diversity involved in iron and cryptic sulfur cycling in the ferruginous, low-sulfate waters of Lake Pavin. *PLoS One* **14**: e0212787.

Blainey, P.C. (2013) The future is now: single-cell genomics of bacteria and archaea. *Fems Microbiol Rev* **37**: 407–427.

Blakemore, R. (1975) Magnetotactic bacteria. *Science* **190**: 377–379.

Bonhomme, C. (2008) Turbulences et ondes en milieu naturel stratifié : deux études de cas : étude du mélange turbulent et des ondes internes du lac Pavin (Auvergne, France) ; influence des ondes de Rossby sur la concentration en chlorophylle de surface dans l'upwelling du Pérou.

Bonhomme, C., Poulin, M., Vincon-Leite, B., Saad, M., Groleau, A., Jezequel, D., and Tassin, B. (2011) Maintaining meromixis in Lake Pavin (Auvergne, France): The key role of a sublacustrine spring. *C R Geosci* **343**: 749–759.

Bura-Nakic, E., Viollier, E., Jezequel, D., Thiam, A., and Ciglenecki, I. (2009) Reduced sulfur and iron species in anoxic water column of meromictic crater Lake Pavin (Massif Central, France). *Chem Geol* **266**: 311–317.

Busigny, V., Jézéquel, D., Cosmidis, J., Viollier, E., Benzerara, K., Planavsky, N.J., et al. (2016) The Iron Wheel in Lac Pavin: Interaction with Phosphorus Cycle. In *Lake*

589 *Pavin: History, geology, biogeochemistry, and sedimentology of a deep meromictic*
590 *maar lake*. Sime-Ngando, T., Boivin, P., Chapron, E., Jezequel, D., and Meybeck, M.
591 (eds). Cham: Springer International Publishing, pp. 205–220.
592 Busigny, V., Planavsky, N.J., Jézéquel, D., Crowe, S., Louvat, P., Moureau, J., et al. (2014)
593 Iron isotopes in an Archean ocean analogue. *Geochimica et Cosmochimica Acta* **133**:
594 443–462.
595 Chapron, E., Alberic, P., Jezequel, D., Versteeg, W., Bourdier, J.-L., and Sitbon, J. (2010)
596 Multidisciplinary characterisation of sedimentary processes in a recent maar lake
597 (Lake Pavin, French Massif Central) and implication for natural hazards. *Nat Hazards*
598 *Earth Syst Sci* **10**: 1815–1827.
599 Cosmidis, J., Benzerara, K., Morin, G., Busigny, V., Lebeau, O., Jezequel, D., et al. (2014)
600 Biomineralization of iron-phosphates in the water column of Lake Pavin (Massif
601 Central, France). *Geochim Cosmochim Acta* **126**: 78–96.
602 Descamps, E.C.T., Monteil, C.L., Menguy, N., Ginet, N., Pignol, D., Bazylinski, D.A., and
603 Lefèvre, C.T. (2017) Desulfamplus magnetovallimortis gen. nov., sp. nov., a
604 magnetotactic bacterium from a brackish desert spring able to biomineralize greigite
605 and magnetite, that represents a novel lineage in the Desulfobacteraceae. *Systematic*
606 *and Applied Microbiology* **40**: 280–289.
607 Flies, C.B., Jonkers, H.M., de Beer, D., Bosselmann, K., Bottcher, M.E., and Schüler, D.
608 (2005) Diversity and vertical distribution of magnetotactic bacteria along chemical
609 gradients in freshwater microcosms. *FEMS Microbiol Ecol* **52**: 185–195.
610 Frankel, R.B., Bazylinski, D.A., Johnson, M.S., and Taylor, B.L. (1997) Magneto-aerotaxis in
611 marine coccoid bacteria. *Biophys J* **73**: 994–1000.
612 Jogler, C., Kube, M., Schübbe, S., Ullrich, S., Teeling, H., Bazylinski, D.A., et al. (2009)
613 Comparative analysis of magnetosome gene clusters in magnetotactic bacteria

provides further evidence for horizontal gene transfer. *Environ Microbiol* **11**: 1267–1277.

Jogler, C., Lin, W., Meyerdierks, A., Kube, M., Katzmann, E., Flies, C., et al. (2009) Toward cloning of the magnetotactic metagenome: identification of magnetosome island gene clusters in uncultivated magnetotactic bacteria from different aquatic sediments. *Appl Environ Microbiol* **75**: 3972–3979.

Jogler, C., Niebler, M., Lin, W., Kube, M., Wanner, G., Kolinko, S., et al. (2010) Cultivation-independent characterization of "Candidatus Magnetobacterium bavaricum" via ultrastructural, geochemical, ecological and metagenomic methods. *Environ Microbiol* **12**: 2466–2478.

Jogler, C. and Schüler, D. (2009) Genomics, genetics, and cell biology of magnetosome formation. *Annu Rev Microbiol* **63**: 501–521.

Kolinko, S., Richter, M., Glöckner, F.-O., Brachmann, A., and Schüler, D. (2016) Single-cell genomics of uncultivated deep-branching magnetotactic bacteria reveals a conserved set of magnetosome genes. *Environ Microbiol* **18**: 21–37.

Kolinko, S., Wanner, G., Katzmann, E., Kiemer, F., Fuchs, B.M., and Schüler, D. (2013) Clone libraries and single cell genome amplification reveal extended diversity of uncultivated magnetotactic bacteria from marine and freshwater environments. *Environ Microbiol* **15**: 1290–1301.

Koziaeva, V.V., Alekseeva, L.M., Uzun, M.M., Leão, P., Sukhacheva, M.V., Patutina, E.O., et al. (2020) Biodiversity of Magnetotactic Bacteria in the Freshwater Lake Beloe Bordukovskoe, Russia. *Microbiology* **89**: 348–358.

Lefèvre, C.T. (2016) Genomic insights into the early-diverging magnetotactic bacteria. *Environ Microbiol* **18**: 1–3.

Lefèvre, C.T. and Bazylinski, D.A. (2013) Ecology, diversity, and evolution of magnetotactic bacteria. *Microbiol Mol Biol Rev* **77**: 497–526.

640 Lefèvre, C.T., Bennet, M., Landau, L., Vach, P., Pignol, D., Bazylinski, D.A., et al. (2014)
641 Diversity of magneto-aerotactic behaviors and oxygen sensing mechanisms in cultured
642 magnetotactic bacteria. *Biophys J* **107**: 527–538.
643 Lefèvre, C.T., Bernadac, A., Yu-Zhang, K., Pradel, N., and Wu, L.-F. (2009) Isolation and
644 characterization of a magnetotactic bacterial culture from the Mediterranean Sea.
645 *Environ Microbiol* **11**: 1646–1657.
646 Lefèvre, C.T., Frankel, R.B., Abreu, F., Lins, U., and Bazylinski, D.A. (2011) Culture-
647 independent characterization of a novel, uncultivated magnetotactic member of the
648 Nitrospirae phylum. *Environ Microbiol* **13**: 538–549.
649 Lefèvre, C.T., Howse, P.A., Schmidt, M.L., Sabaty, M., Menguy, N., Luther, G.W., and
650 Bazylinski, D.A. (2016) Growth of magnetotactic sulfate-reducing bacteria in oxygen
651 concentration gradient medium. *Environ Microbiol Rep* **8**: 1003–1015.
652 Lefèvre, C.T., Schmidt, M.L., Viloria, N., Trubitsyn, D., Schüler, D., and Bazylinski, D.A.
653 (2012) Insight into the evolution of magnetotaxis in Magnetospirillum spp., based on
654 mam gene phylogeny. *Appl Environ Microbiol* **78**: 7238–7248.
655 Li, J., Ge, X., Zhang, X., Chen, G., and Pan, Y. (2010) Recover vigorous cells of
656 Magnetospirillum magneticum AMB-1 by capillary magnetic separation. *Chin J*
657 *Ocean Limnol* **28**: 826–831.
658 Li, J., Liu, P., Wang, J., Roberts, A.P., and Pan, Y. (2020c) Magnetotaxis as an Adaptation to
659 Enable Bacterial Shuttling of Microbial Sulfur and Sulfur Cycling Across Aquatic
660 Oxic-Anoxic Interfaces. *J Geophys Res-Biogeosci* **125**: e2020JG006012.
661 Li, J., Menguy, N., Gatel, C., Boureau, V., Snoeck, E., Patriarche, G., et al. (2015) Crystal
662 growth of bullet-shaped magnetite in magnetotactic bacteria of the Nitrospirae
663 phylum. *J R Soc Interface* **12**:.
664 Li, J., Menguy, N., Leroy, E., Roberts, A.P., Liu, P., and Pan, Y. (2020a) Biomineralization
665 and Magnetism of Uncultured Magnetotactic Coccus Strain THC-1 With Non-chained

Magnetosomal Magnetite Nanoparticles. *Journal of Geophysical Research: Solid Earth* **125**: e2020JB020853.

Li, J., Menguy, N., Roberts, A.P., Gu, L., Leroy, E., Bourgon, J., et al. (2020b) Bullet-Shaped Magnetite Biomineralization Within a Magnetotactic Deltaproteobacterium: Implications for Magnetofossil Identification. *Journal of Geophysical Research: Biogeosciences* **125**: e2020JG005680.

Li, J., Zhang, H., Liu, P., Menguy, N., Roberts, A.P., Chen, H., et al. (2019) Phylogenetic and Structural Identification of a Novel Magnetotactic Deltaproteobacteria Strain, WYHR-1, from a Freshwater Lake. *Appl Environ Microbiol* **85**:.

Li, J., Zhang, H., Menguy, N., Benzerara, K., Wang, F., Lin, X., et al. (2017) Single-Cell Resolution of Uncultured Magnetotactic Bacteria via Fluorescence-Coupled Electron Microscopy. *Appl Environ Microbiol* **83**: pii: e00409-17.

Lin, W., Li, J., and Pan, Y. (2012) Newly isolated but uncultivated magnetotactic bacterium of the phylum Nitrospirae from Beijing, China. *Appl Environ Microbiol* **78**: 668–675.

Lin, W., Pan, Y., and Bazylinski, D.A. (2017) Diversity and ecology of and biomineralization by magnetotactic bacteria. *Environ Microbiol Rep* **9**: 345–356.

Lin, W., Tian, L., Li, J., and Pan, Y. (2008) Does capillary racetrack-based enrichment reflect the diversity of uncultivated magnetotactic cocci in environmental samples? *FEMS Microbiol Lett* **279**: 202–206.

Lin, W., Wang, Y., Gorby, Y., Nealson, K., and Pan, Y. (2013) Integrating niche-based process and spatial process in biogeography of magnetotactic bacteria. *Sci Rep* **3**: 1643.

Lin, W., Zhang, W., Zhao, X., Roberts, A.P., Paterson, G.A., Bazylinski, D.A., and Pan, Y. (2018) Genomic expansion of magnetotactic bacteria reveals an early common origin of magnetotaxis with lineage-specific evolution. *ISME J* **12**: 1508–1519.

691 Lins, U., Freitas, F., Keim, C.N., Barros, H.L. de, Esquivel, D.M.S., and Farina, M. (2003)
692 Simple homemade apparatus for harvesting uncultured magnetotactic microorganisms.
693 *Brazilian Journal of Microbiology* **34**: 111–116.
694 Liu, J., Zhang, W., Du, H., Leng, X., Li, J.-H., Pan, H., et al. (2018) Seasonal changes in the
695 vertical distribution of two types of multicellular magnetotactic prokaryotes in the
696 sediment of Lake Yuehu, China. *Environ Microbiol Rep* **10**: 475–484.
697 Liu, P., Liu, Y., Zhao, X., Roberts, A.P., Zhang, H., Zheng, Y., et al. (2020) Diverse
698 phylogeny and morphology of magnetite biomineralized by magnetotactic cocci.
699 *Environ Microbiol*.
700 Lopes, F., Viollier, E., Thiam, A., Michard, G., Abril, G., Groleau, A., et al. (2011)
701 Biogeochemical modelling of anaerobic vs. aerobic methane oxidation in a
702 meromictic crater lake (Lake Pavin, France). *Appl Geochem* **26**: 1919–1932.
703 Michard, G., Viollier, E., Jézéquel, D., and Sarazin, G. (1994) Geochemical study of a crater
704 lake: Pavin Lake, France — Identification, location and quantification of the chemical
705 reactions in the lake. *Chemical Geology* **115**: 103–115.
706 Miot, J., Jezequel, D., Benzerara, K., Cordier, L., Rivas-Lamelo, S., Skouri-Panet, F., et al.
707 (2016) Mineralogical Diversity in Lake Pavin: Connections with Water Column
708 Chemistry and Biomineralization Processes. *Minerals* **6**: UNSP 24.
709 Monteil, C.L., Benzerara, K., Menguy, N., Bidaud, C.C., Michot-Achdjian, E., Bolzoni, R., et
710 al. (2021) Intracellular amorphous Ca-carbonate and magnetite biomineralization by a
711 magnetotactic bacterium affiliated to the Alphaproteobacteria. *The ISME Journal* **15**:
712 1–18.
713 Monteil, C.L. and Lefevre, C.T. (2019) Magnetoreception in Microorganisms. *Trends in*
714 *Microbiology* **0**:.

715 Monteil, C.L., Vallenet, D., Menguy, N., Benzerara, K., Barbe, V., Fouteau, S., et al. (2019)
716 Ectosymbiotic bacteria at the origin of magnetoreception in a marine protist. *Nat*
717 *Microbiol* **4**: 1088–1095.
718 Moskowitz, B.M., Bazylinski, D.A., Egli, R., Frankel, R.B., and Edwards, K.J. (2008)
719 Magnetic properties of marine magnetotactic bacteria in a seasonally stratified coastal
720 pond (Salt Pond, MA, USA). *Geophys J Int* **174**: 75–92.
721 Oestreicher, Z., Lower, S., and Lower, B. (2011) Magnetotactic Bacteria Containing
722 Phosphorus-Rich Inclusion Bodies. *Microscopy and Microanalysis* **17**: 140–141.
723 Pan, H., Dong, Y., Teng, Z., Li, J., Zhang, W., Xiao, T., and Wu, L.-F. (2019) A species of
724 magnetotactic deltaproteobacterium was detected at the highest abundance during an
725 algal bloom. *FEMS Microbiol Lett* **366**:.
726 Popp, F., Armitage, J.P., and Schüler, D. (2014) Polarity of bacterial magnetotaxis is
727 controlled by aerotaxis through a common sensory pathway. *Nat Commun* **5**: 5398.
728 Qian, X.-X., Santini, C.-L., Kosta, A., Menguy, N., Le Guenno, H., Zhang, W., et al. (2020)
729 Juxtaposed membranes underpin cellular adhesion and display unilateral cell division
730 of multicellular magnetotactic prokaryotes. *Environ Microbiol* **22**: 1481–1494.
731 R Core Team (2018) R: A language and environment for statistical computing. R Foundation
732 for Statistical Computing, Vienna, Austria. URL https://www.R-project.org/. *R*
733 *Foundation for Statistical Computing, Vienna, Austria*.
734 Rivas-Lamelo, S., Benzerara, K., Lefèvre, C.T., Jézéquel, D., Menguy, N., Viollier, E., et al.
735 (2017) Magnetotactic bacteria as a new model for P sequestration in the ferruginous
736 Lake Pavin. *Geochemical Perspectives Letters* **5**: 35–41.
737 Schettler, G., Schwab, M.J., and Stebich, M. (2007) A 700-year record of climate change
738 based on geochemical and palynological data from varved sediments (Lac Pavin,
739 France). *Chem Geol* **240**: 11–35.

740 Schüler, D. (2002) The biomineralization of magnetosomes in Magnetospirillum
741 gryphiswaldense. *Int Microbiol* **5**: 209–214.
742 Schulz-Vogt, H.N., Pollehne, F., Jürgens, K., Arz, H.W., Beier, S., Bahlo, R., et al. (2019)
743 Effect of large magnetotactic bacteria with polyphosphate inclusions on the phosphate
744 profile of the suboxic zone in the Black Sea. *ISME J* **13**: 1198–1208.
745 Simmons, S.L., Bazylinski, D.A., and Edwards, K.J. (2007) Population dynamics of marine
746 magnetotactic bacteria in a meromictic salt pond described with qPCR. *Environ*
747 *Microbiol* **9**: 2162–2174.
748 Simmons, S.L., Sievert, S.M., Frankel, R.B., Bazylinski, D.A., and Edwards, K.J. (2004)
749 Spatiotemporal distribution of marine magnetotactic bacteria in a seasonally stratified
750 coastal salt pond. *Appl Environ Microbiol* **70**: 6230–6239.
751 Spring, S., Amann, R., Ludwig, W., Schleifer, K.H., Schuler, D., Poralla, K., and Petersen, N.
752 (1994) Phylogenetic analysis of uncultured magnetotactic bacteria from the alpha-
753 subclass of Proteobacteria. *Syst Appl Microbiol* **17**: 501–508.
754 Spring, S., Amann, R., Ludwig, W., Schleifer, K.H., Vangemerden, H., and Petersen, N.
755 (1993) Dominating role of an unusual magnetotactic bacterium in the microaerobic
756 zone of a fresh-water sediment. *Appl Environ Microbiol* **59**: 2397–2403.
757 Viollier, E., Jezequel, D., Michard, G., Pepe, M., Sarazin, G., and Alberic, P. (1995)
758 Geochemical Study of a Crater Lake (pavin Lake, France) - Trace-Element Behavior
759 in the Monimolimnion. *Chem Geol* **125**: 61–72.
760 Wolfe, R.S., Thauer, R.K., and Pfennig, N. (1987) A ‘capillary racetrack’ method for
761 isolation of magnetotactic bacteria. *FEMS Microbiology Letters* **45**: 31–35.
762 Xiao, Z., Lian, B., Chen, J., and Teng, H.H. (2007) Design and application of the method for
763 isolating magnetotactic bacteria. *Chin J Geochem* **26**: 252–258.

764 Zhang, H., Menguy, N., Wang, F., Benzerara, K., Leroy, E., Liu, P., et al. (2017)
765 Magnetotactic Coccus Strain SHHC-1 Affiliated to Alphaproteobacteria Forms
766 Octahedral Magnetite Magnetosomes. *Front Microbiol* **8**:.
767
768
769

Figure and Figure legends

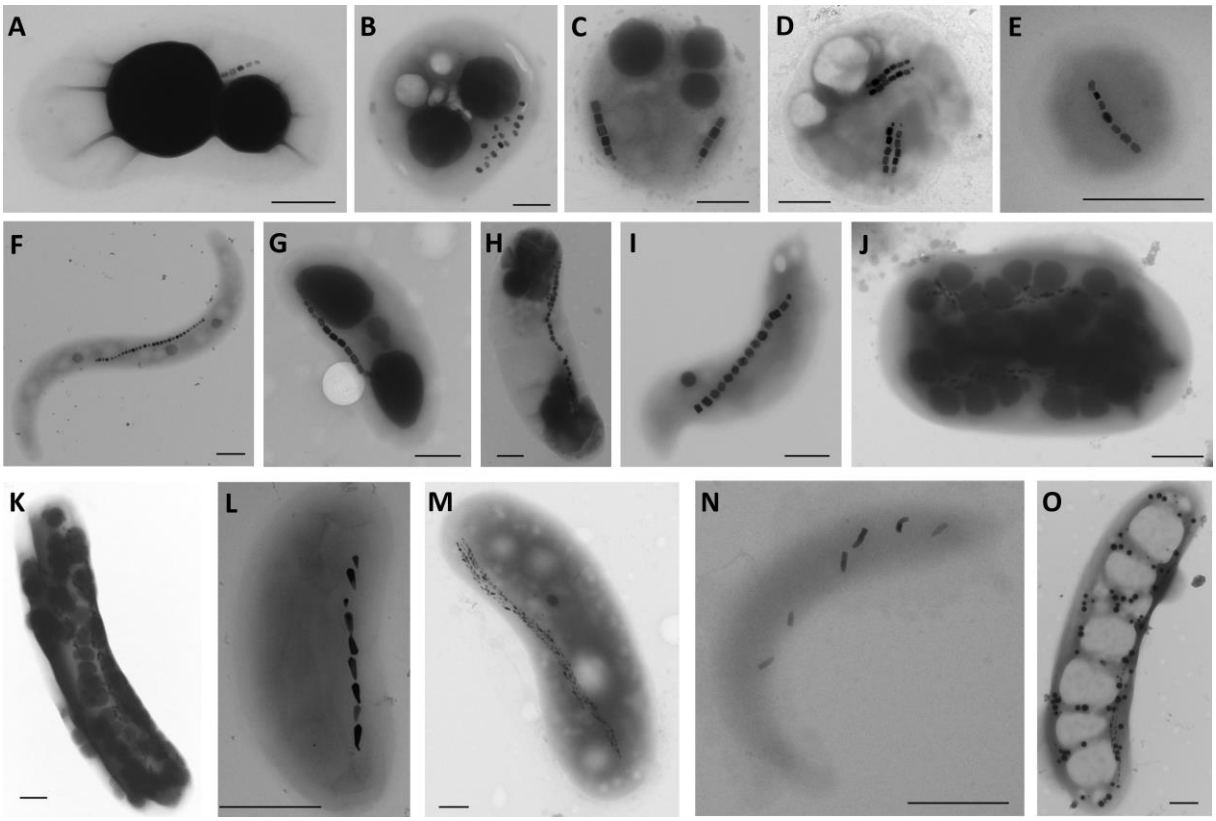

Fig. 1. Transmission electron microscope images of different magnetotactic bacteria morphotypes observed in Lake Pavin sediments. See main text for morphotypes description. Scale bars represent 0.5 µm.

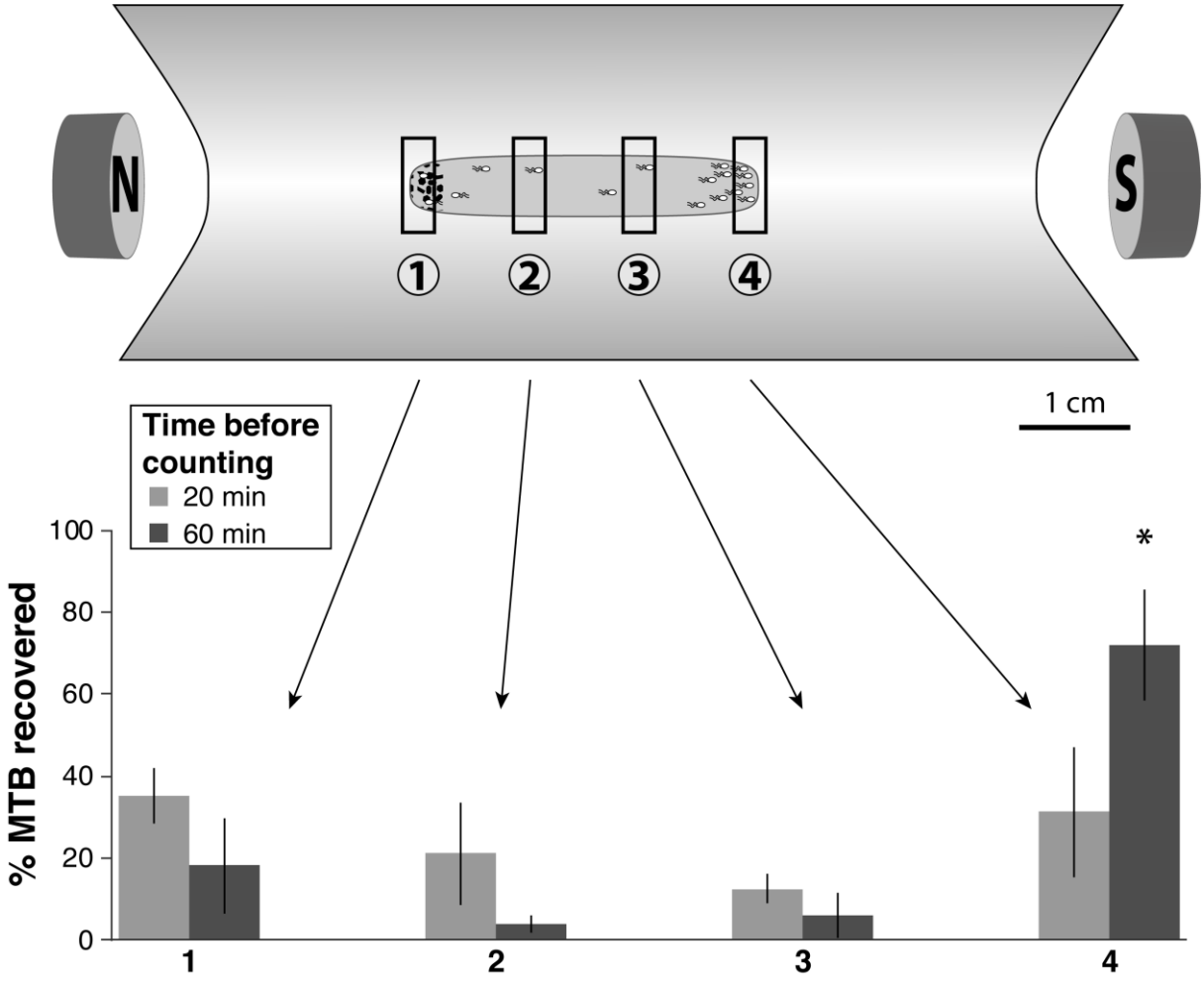

Fig. 2. Magnetic purification of MTB from Lake Pavin sediments using the migration track device, developed in the present work. The pellet of magnetically enriched cells is deposited on the left side of the system (*i.e.* position 1) and magnetic particles (represented by the black dots) and south seeking MTB are trapped by the left magnetic bar. North seeking MTB swim toward the right magnetic bar with the majority accumulating at position 4. Histograms on the lower part of the figure represent the proportion of cells counted at each position (1, 2, 3 and 4) after 20 or 60 min of magnetic purification, illustrating the efficiency of our migration track device. Cell counts are reported as the mean of triplicate measurements, with vertical lines indicating 2σ uncertainties. The zone 4 after 60 min of magnetic purification is the only condition that concentrates significantly MTB relative to others. This is supported by a pairwise student t-test ($p < 0.034$).

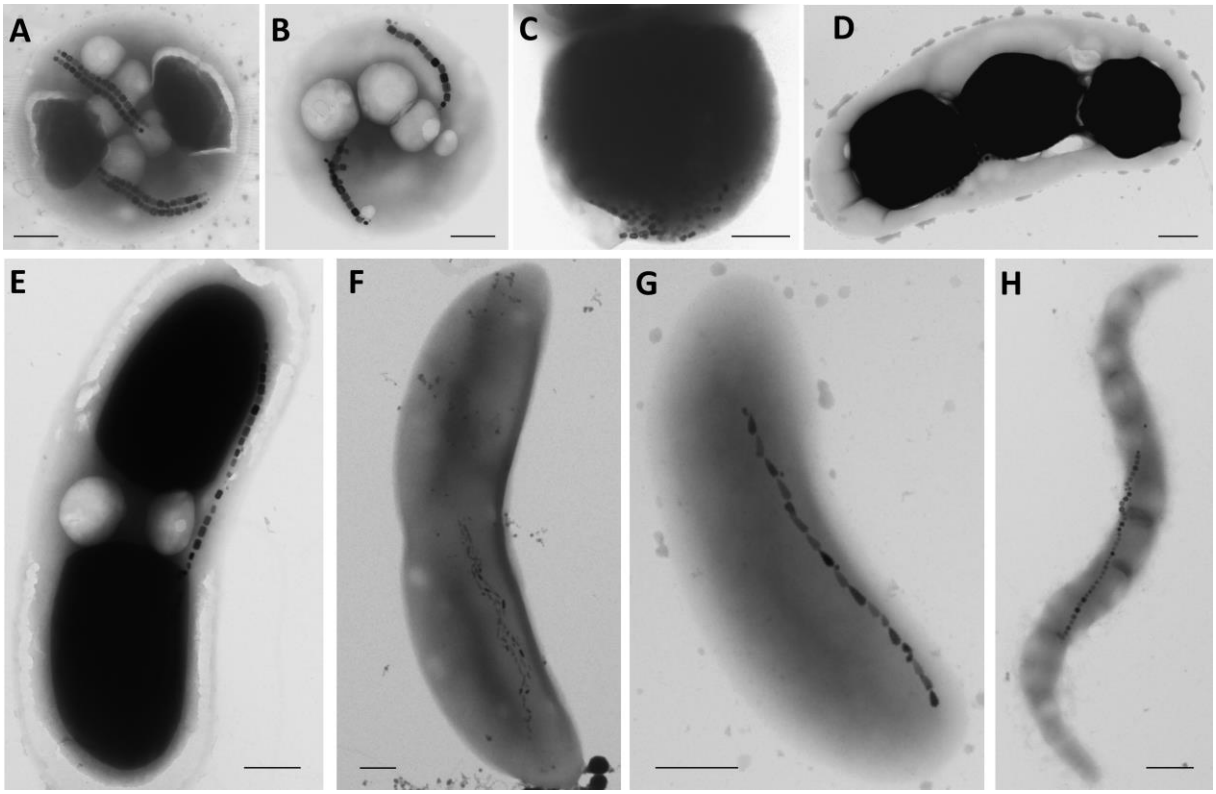

Fig. 3. Transmission electron microscope images of different magnetotactic bacteria morphotypes from Lake Pavin water column. See main text for morphotypes description. Scale bars represent 0.5 µm.

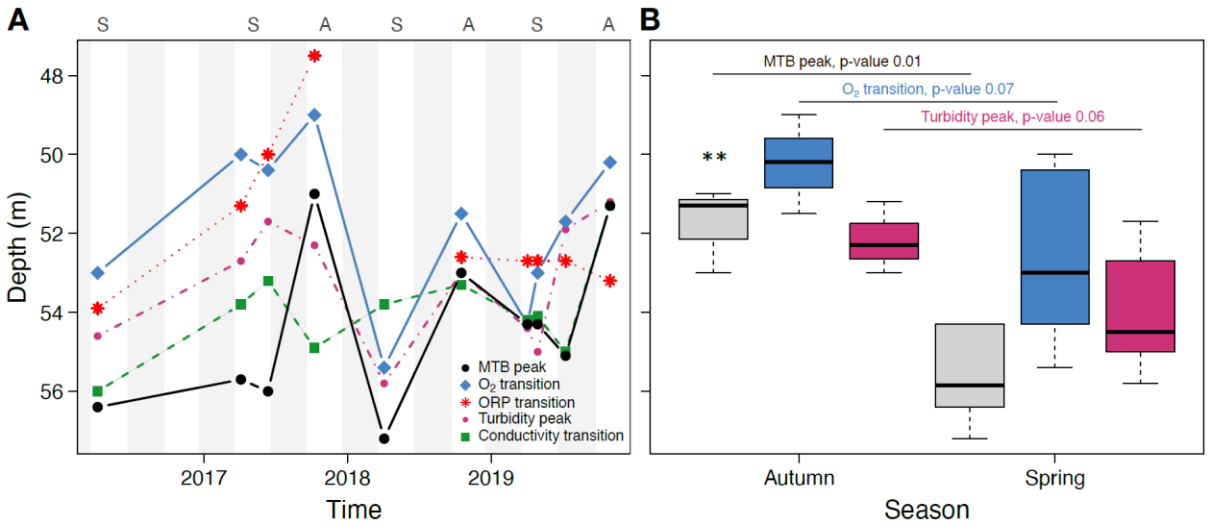

796

797 **Fig. 4.** A) Depth variations of the MTB and turbidity peaks, as well as conductivity, oxygen
798 and redox potential transitions upper boundarie (*i.e.* depth where the maximum gradient starts)
799 over time. B) Box plots showing the distribution of these depths as a function of the sampling
800 season for the variables with the most significant mean differences according to a pairwise
801 Student's t-test ($p < 0.1$).

802

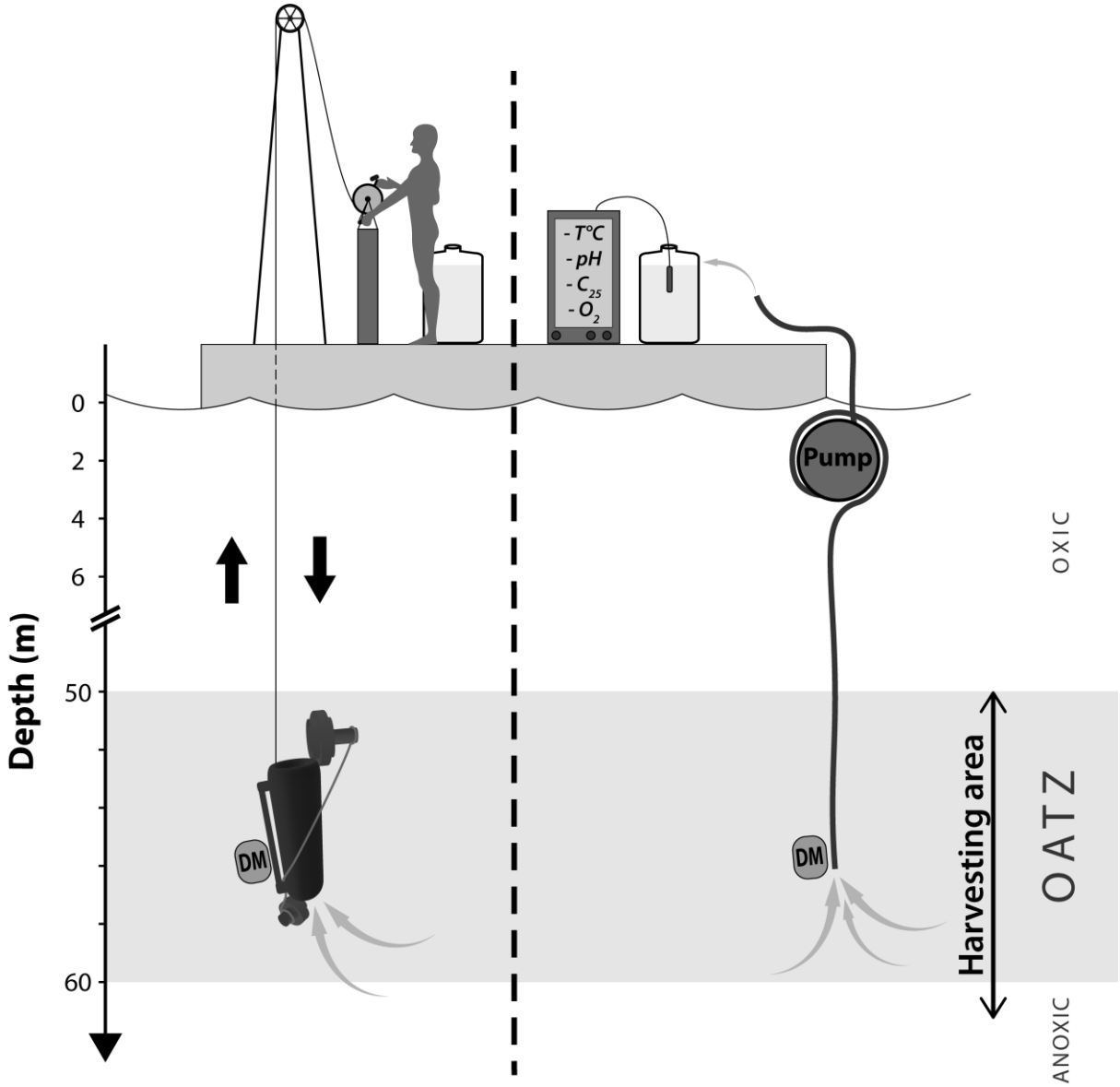

803

804 **Fig. 5.** Schematic representation of the methods used to sample the water column of Lake Pavin
805 using a Niskin bottle (left side) and online pumping (right side). DM refers to the depthmeter
806 used to control the pipe depth. The oxic-anoxic transition zone (OATZ) represents the region
807 where oxygen concentrations are at the micromolar to sub-micromolar levels and where
808 populations of magnetotactic cells are present.

809

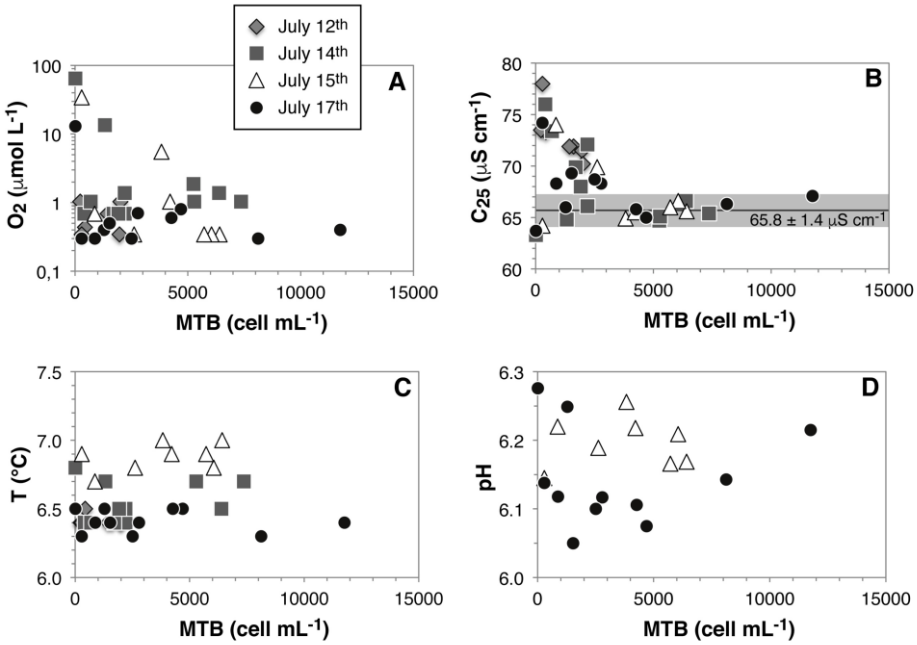

Fig. 6. Relations between MTB cell abundance and various physicochemical parameters from Lake Pavin water column in the vicinity of the redox boundary, during the July 2019 sampling campaign. (A) Dissolved oxygen concentration (µmol L^{-1}), (B) specific conductivity at 25°C (µS cm^{-1}), (C) temperature (°C), and (D) pH. All samples were collected with our online pumping system (Fig. 5 left panel). Note that the temperature measured on the platform could slightly differ from the temperature at depth (i.e. approximately 4°C (Michard *et al.*, 1994; Bonhomme *et al.*, 2011)) due to thermal exchange in the 60-m long pipe.

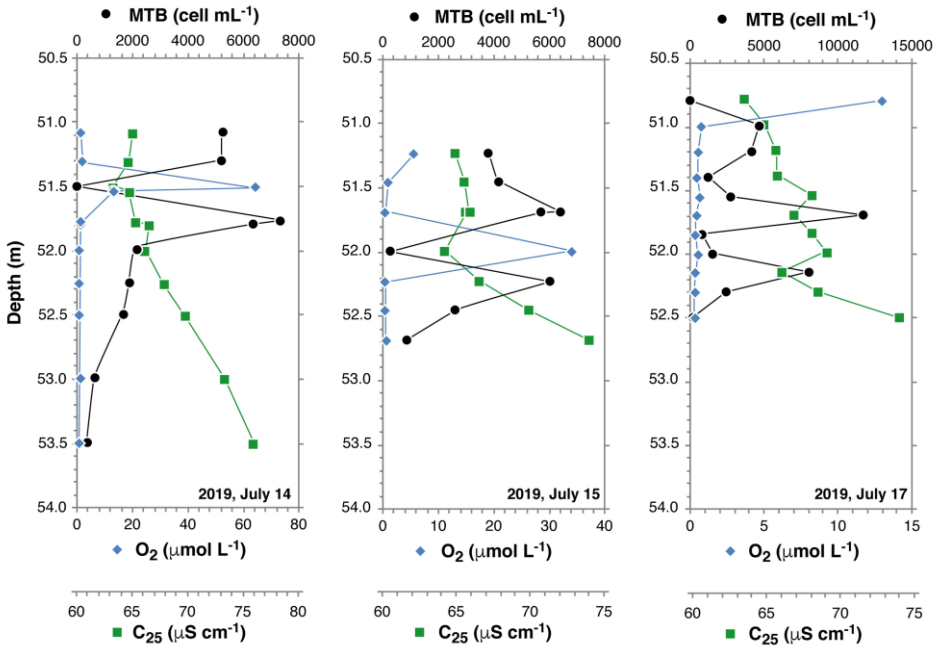

819

820 **Fig. 7.** Magnetotactic cell abundance (cell mL^{-1}), dissolved oxygen concentration (µmol L^{-1})
821 and specific conductivity (µS cm^{-1}) profiles from Lake Pavin water column, on July 14th, 15th
822 and 17th 2019. The high-spatial resolution of water collection was reached using online
823 collecting system.

824

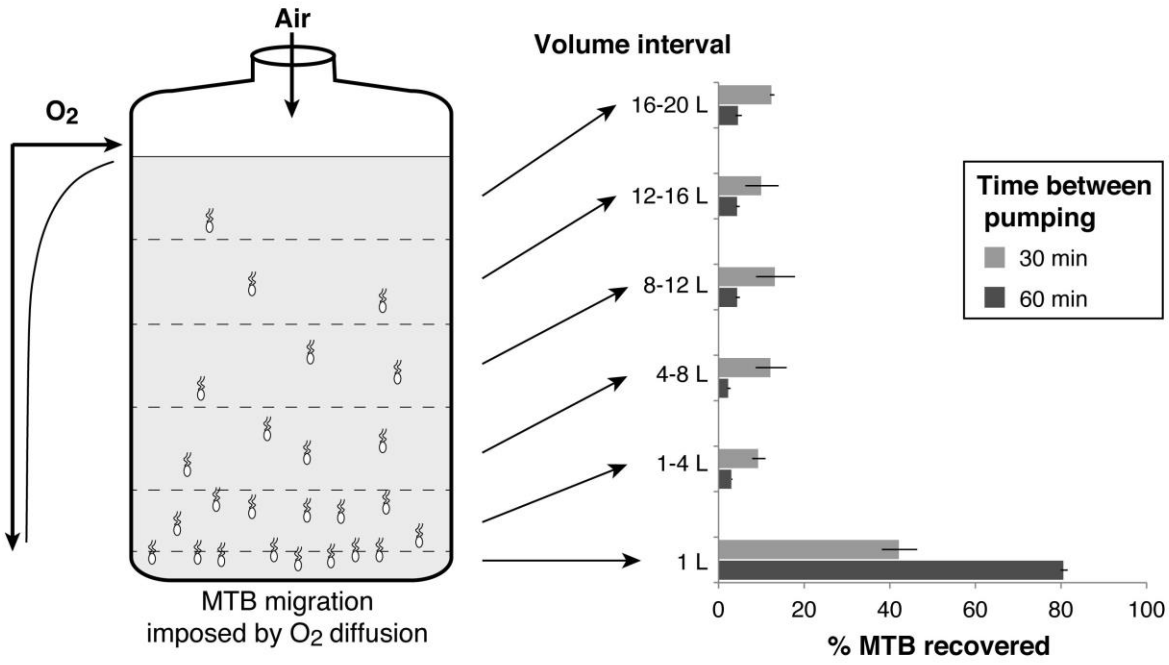

825

826 **Fig. 8.** Schematic representation (left panel) of the aerotactic concentration of magnetotactic
827 bacteria after collection from the water column with the online pumping system and transferred
828 in a 20-L Nalgene bottle. Histograms (right panel) represent the percentage of MTB cells
829 recovered in each water layer after 30 or 60 min of idle time between pumping, showing the
830 efficiency of our device. The percentage of MTB recovered are reported as the mean of
831 triplicate counts and line extensions represent the positive and negative standard deviations.
832 The thickness of each water layer in the Nalgene bottle was about 10 cm.

833

Supporting Information

Mass collection of magnetotactic bacteria from the permanently stratified ferruginous Lake Pavin, France

Vincent Busigny[1,2,*], François P. Mathon[1,3], Didier Jézéquel[1,4], Cécile C. Bidaud[5], Eric Viollier[1], Gérard Bardoux[1], Jean-Jacques Bourrand[1], Karim Benzerara[5], Elodie Duprat[5], Nicolas Menguy[5], Caroline L. Monteil[3], Christopher T. Lefevre[3,*]

[1]Université de Paris, Institut de Physique du Globe de Paris, CNRS, F-75005, Paris, France

[2]Institut Universitaire de France, 75005 Paris, France

[3]Aix-Marseille University, CNRS, CEA, UMR7265 Institute of Biosciences and Biotechnologies of Aix-Marseille, CEA Cadarache, F-13108 Saint-Paul-lez-Durance, France

[4]INRAE & Université Savoie Mont Blanc, UMR CARRTEL, 74200 Thonon-les-Bains, France

[5]Sorbonne Université, Muséum National d'Histoire Naturelle, UMR CNRS 7590, IRD. Institut de Minéralogie, de Physique des Matériaux et de Cosmochimie (IMPMC), Paris, France.

*For correspondence. E-mails: busigny@ipgp.fr, christopher.lefevre@cea.fr

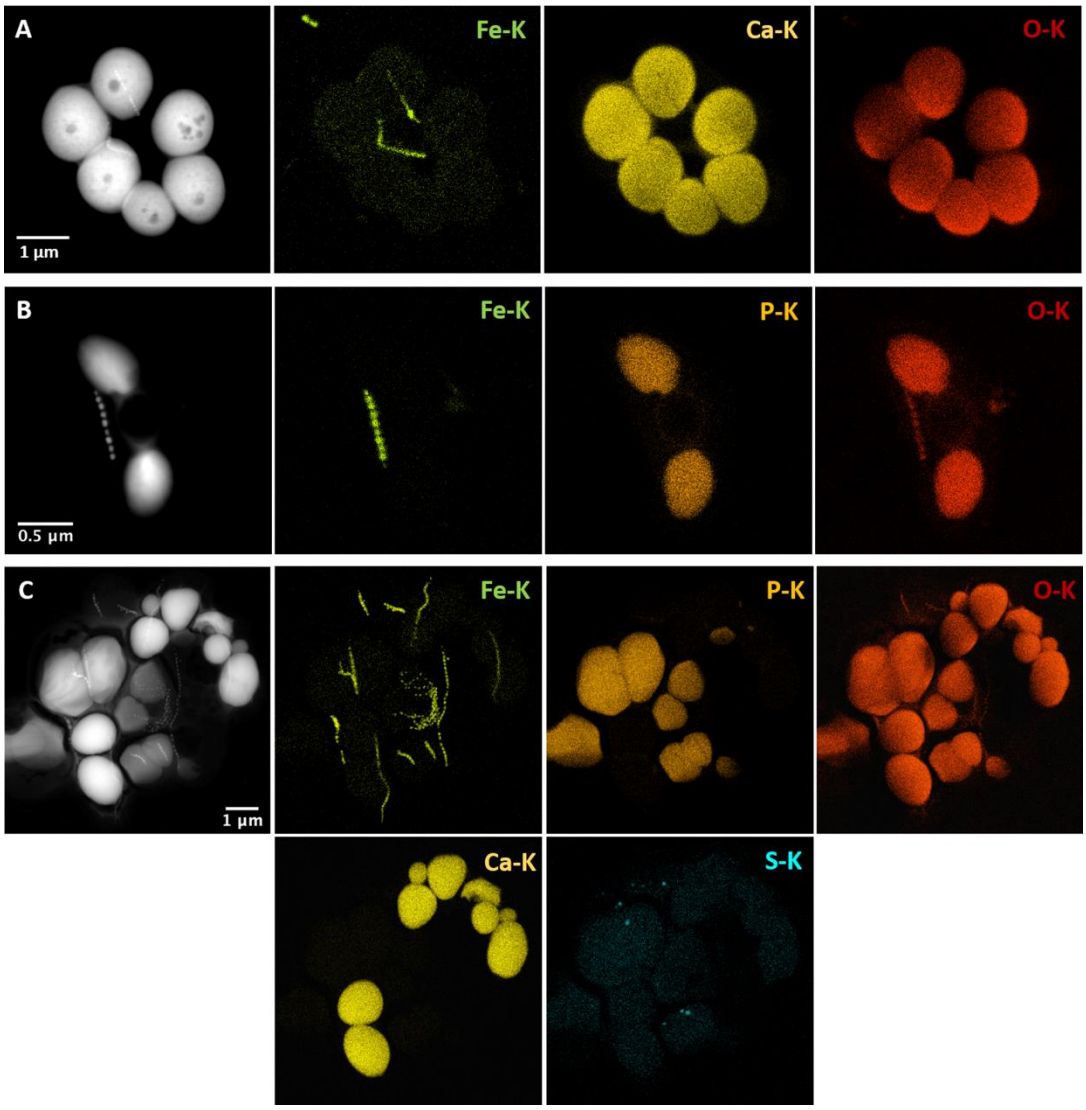

Fig. S1. Z-contrast imaging in the high-angle annular dark field (STEM-HAADF) mode, and elemental mapping by X-ray energy-dispersive spectrometry (XEDS) showing the chemical composition of inclusions formed by magnetotactic bacteria present in the sediments (A and B) and in the water column (C) of Lake Pavin.

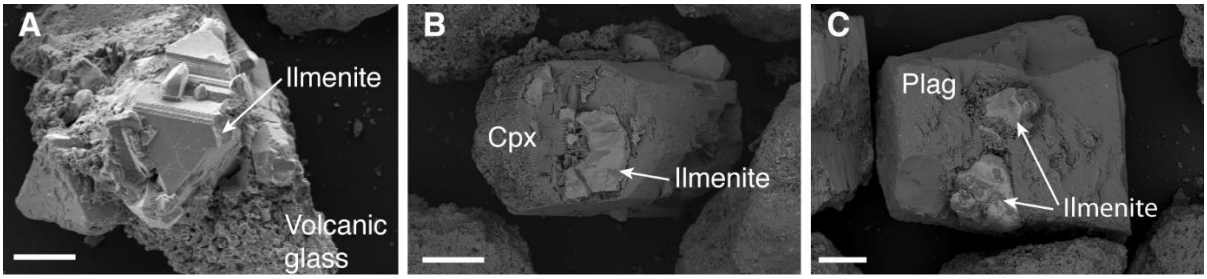

Fig. S2. Scanning electron microscope images of ilmenite inclusions in volcanic glass (A), and clinopyroxene (Cpx) (B) and plagioclase (Plag) (C) crystals. This illustrates the volcanic origin of ilmenite from Lake Pavin sediments. Scale bars represent 100 µm.

Fig. S3. Picture of the migration track system. Edges of the drop exposed to a magnetic field generated by the two disc magnets are shown by arrows. The scale is shown by a ruler.

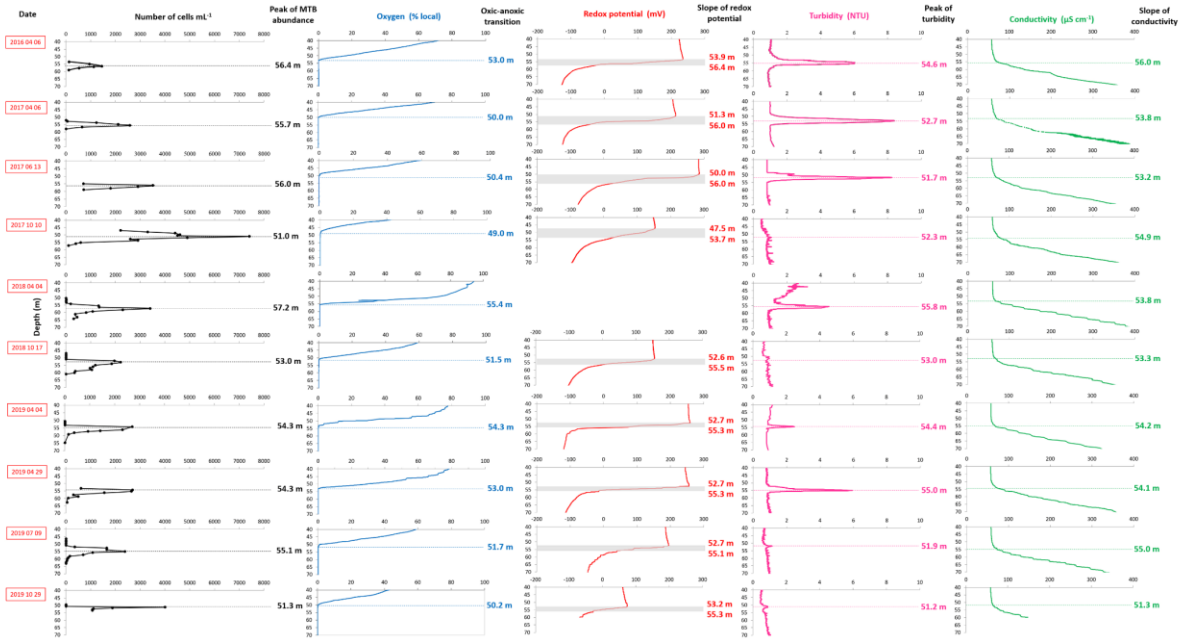
Date
Number of cells mL⁻¹
Peak of MTB abundance
Oxygen (% local)
Oxic-anoxic transition
Redox potential (mV)
Slope of redox potential
Turbidity (NTU)
Peak of turbidity
Conductivity (µS cm⁻¹)
Slope of conductivity
Depth (m)
2016 04 06
2017 04 06
2017 06 13
2017 10 10
2018 04 04
2018 10 17
2019 04 04
2019 04 29
2019 07 09
2019 10 29
56.4 m
55.7 m
56.0 m
51.0 m
57.2 m
53.0 m
54.3 m
54.3 m
55.1 m
51.3 m
53.0 m
50.0 m
50.4 m
49.0 m
55.4 m
51.5 m
54.3 m
53.0 m
51.7 m
50.2 m
53.9 m
56.4 m
51.3 m
56.0 m
50.0 m
56.0 m
47.5 m
53.7 m
52.6 m
55.5 m
52.7 m
55.3 m
52.7 m
55.3 m
52.7 m
55.1 m
53.2 m
55.3 m
54.6 m
52.7 m
51.7 m
52.3 m
55.8 m
53.0 m
54.4 m
55.0 m
51.9 m
51.2 m
56.0 m
53.8 m
53.2 m
54.9 m
53.8 m
53.3 m
54.2 m
54.1 m
55.0 m
51.3 m

872

873

Fig. S4. Vertical profiles of magnetotactic cells abundance (A), dissolved oxygen concentration (B), redox potential (C), turbidity (D) and conductivity (C_{25}) (E) through the water column. Sampling campaigns were carried out at ten different dates between April 2016 and October 2019. Note that measurements extend through the oxic-anoxic interface and the deeper regions of the anaerobic zone of the water column. Samples used for magnetotactic cells counting were collected using a Niskin bottle. All other parameters correspond to continuous profiles measured using *in situ* probes.

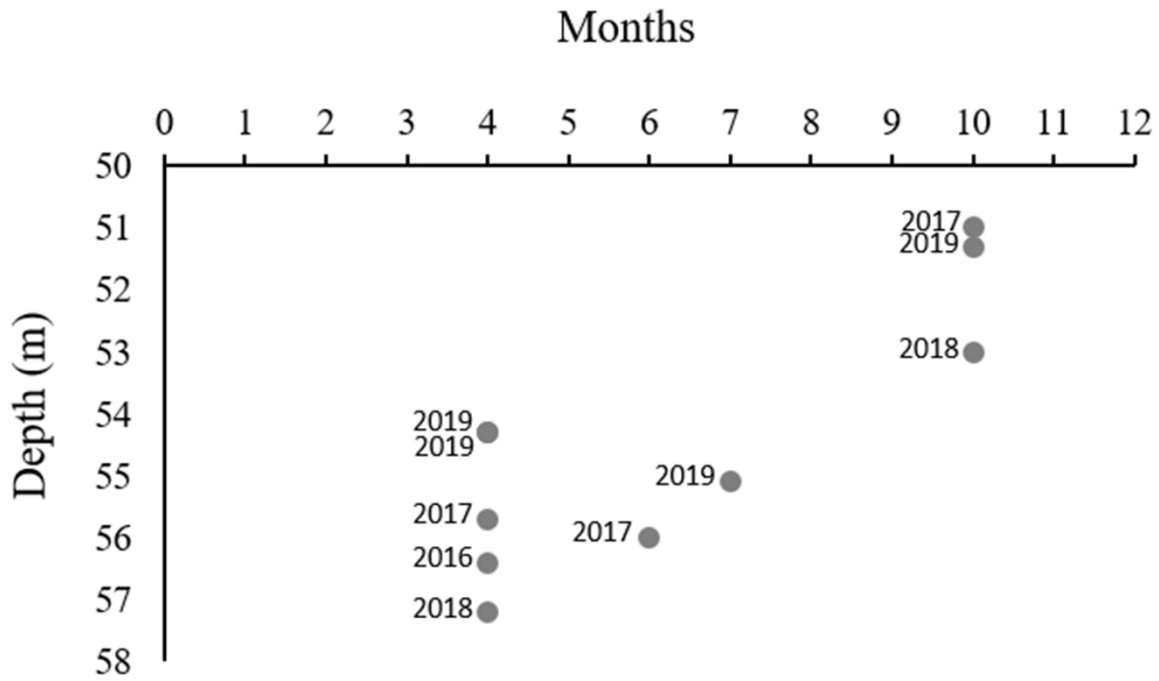

881

882 **Fig. S5.** Depth of the maximum abundance of MTB counted in the water column of Lake Pavin
883 as a function of the month. It illustrates that MTB are generally located shallower in the water
884 column in autumn compared to spring and summer.

885

886